

Influence of nonmagnetic Al ions on magnetoresistance of double-perovskite $\text{Sr}_{2-x}\text{Al}_x\text{MoO}_6$ ($0 \leq x \leq 0.30$)

Yu Sui, Xianjie Wang, Jinguang Cheng, Zhiguo Liu, Jipeng Miao, Xiqiang Huang, Zhe Lu, Zhengnan Qian, Wenhui Su, Jinke Tang, and C. K. Ong

Citation: *Journal of Applied Physics* **98**, 064505 (2005); doi: 10.1063/1.2060936

View online: <http://dx.doi.org/10.1063/1.2060936>

View Table of Contents: <http://scitation.aip.org/content/aip/journal/jap/98/6?ver=pdfcov>

Published by the [AIP Publishing](#)

Articles you may be interested in

[Exchange bias and memory effect in double perovskite \$\text{Sr}_2\text{FeCoO}_6\$](#)
Appl. Phys. Lett. **101**, 142401 (2012); 10.1063/1.4756792

[Effect of La doping on the properties of \$\text{Sr}_{2-x}\text{La}_x\text{FeMoO}_6\$ double perovskite](#)
J. Appl. Phys. **104**, 123903 (2008); 10.1063/1.3043586

[Physical properties of disordered double-perovskite \$\text{Ca}_{2-x}\text{La}_x\text{FeIrO}_6\$](#)
J. Appl. Phys. **103**, 07F716 (2008); 10.1063/1.2830719

[Coexistence of intrinsic and extrinsic magnetoresistance in the double-perovskite \$\text{Sr}_2\text{Fe}\(\text{Mo}_{1-x}\text{W}_x\)\text{O}_{6-w}\$ system](#)
Appl. Phys. Lett. **78**, 2736 (2001); 10.1063/1.1366357

[Grain-boundary room-temperature low-field magnetoresistance in \$\text{Sr}_2\text{FeMoO}_6\$ films](#)
J. Appl. Phys. **87**, 6761 (2000); 10.1063/1.372833



Influence of nonmagnetic Al ions on magnetoresistance of double-perovskite $\text{Sr}_2\text{Fe}_{1-x}\text{Al}_x\text{MoO}_6$ ($0 \leq x \leq 0.30$)

Yu Sui

Center for Condensed Matter Science and Technology (CCMST), Department of Applied Physics, Harbin Institute of Technology, Harbin 150001, People's Republic of China and International Centre for Materials Physics, Chinese Academy of Sciences, Shenyang, 110016, People's Republic of China

Xianjie Wang, Jinguang Cheng, Zhiguo Liu, Jipeng Miao, Xiqiang Huang, Zhe Lu, and Zhengnan Qian

Center for Condensed Matter Science and Technology (CCMST), Department of Applied Physics, Harbin Institute of Technology, Harbin 150001, People's Republic of China

Wenhui Su^{a)}

Center for Condensed Matter Science and Technology (CCMST), Department of Applied Physics, Harbin Institute of Technology, Harbin 150001, People's Republic of China and International Centre for Materials Physics, Chinese Academy of Sciences, Shenyang, 110016, People's Republic of China

Jinke Tang

Department of Physics, University of New Orleans, New Orleans, Louisiana 70148

C. K. Ong

Center for Superconducting and Magnetic Materials and Department of Physics, National University of Singapore, 2 Science Drive 3, Singapore 117542, Singapore

(Received 24 June 2005; accepted 13 August 2005; published online 26 September 2005)

The structural, magnetic, and magnetoresistance properties of the double-perovskite series $\text{Sr}_2\text{Fe}_{1-x}\text{Al}_x\text{MoO}_6$ ($0 \leq x \leq 0.30$) were systematically investigated in order to clarify the influence of nonmagnetic Al ions on the magnetoresistance. The structural refinements of these samples show that the degree of cationic order increases gradually from 88.5% for $x=0$ to 92% for $x=0.30$ without any change in the crystal structure. The magnetization measurements reveal that the substitution of nonmagnetic Al ion for Fe ion enhances the magnetic moment per Fe ion significantly. In addition, the magnetic-field dependence of magnetization and magnetoresistance of these $\text{Sr}_2\text{Fe}_{1-x}\text{Al}_x\text{MoO}_6$ samples were all fitted excellently by taking into account the contributions from ferromagnetic-coupled Fe–O–Mo region and nonferromagnetic-coupled regions. The fitting results indicate that the low-field magnetoresistance can be greatly enhanced due to the separation of the cationic-ordered Fe–O–Mo regions by the paramagnetic Mo–O–Al–O–Mo chains introduced through Al doping. Furthermore, doping nonmagnetic Al ions also suppress the formation of antiferromagnetic Fe–O–Fe antiphase boundaries, and then lead to the improvement of cation ordering and the reduction of magnetoresistance under high field. © 2005 American Institute of Physics. [DOI: 10.1063/1.2060936]

I. INTRODUCTION

Recently, much more attention has been paid on the magnet-transport properties of mixed-valent manganites,¹ half-metallic chromium dioxide,² ordered double-perovskite $\text{Sr}_2\text{FeMoO}_6$ (Ref. 3), etc., due to their promising expectations for spin electronic devices. Especially, for the compound $\text{Sr}_2\text{FeMoO}_6$, due to its half-metallic character and high-magnetic-transition temperature, it exhibits a large room-temperature low-field magnetoresistance (LFMR), which is commonly considered to arise from the spin-dependent carrier scattering at grain boundary.^{3,4} Many schemes for enhancing the magnitude of the LFMR effect in $\text{Sr}_2\text{FeMoO}_6$ (SFMO) have been tested, such as reducing the

grain size⁴ using grain boundary of bicrystal⁵ and introducing the second phase of SrMoO_4 at the grain boundaries.⁶

The magnetic structure of double-perovskite $\text{Sr}_2\text{FeMoO}_6$ was generally described as ferrimagnetic due to the antiferromagnetic coupling of localized up spin electron of Fe^{3+} ($3d^5:t_{2g}^3e_g^2$) and itinerant down spin electron of Mo^{5+} ($4d^1:t_{2g}^1$), but most of the saturated moment per formula unit (M_S) of bulk SFMO reported so far are much smaller than its expected value of $4\mu_B$.^{7–13} This effect was attributed to the presence of antisite defects introduced by the partial disorder of Fe and Mo ions between the B' and B'' sublattices.^{7–13} Goodenough and Dass¹⁴ had suggested that, in sintered polycrystalline SFMO compound, such antisite defects^{15,16} are likely to form the nonrandom disorders, such as antiphase boundaries (APBs), which were directly observed by high-resolution electron microscopy.^{15–17} The influence of Fe/Mo

^{a)} Author to whom correspondence should be addressed; electronic mail: suiyu@hit.edu.cn

disorder (antisite defects) on magnetoresistance and magnetization in the double perovskite were well documented in Refs. 8–13. It has been shown that with the increase of the antisite defect concentration (or APBs) the magnetization decreases almost linearly due to the antiferromagnetic-coupled Fe–O–Fe in the APBs.^{8,10,13} In addition, the high-field MR (HFMR) observed in bulk SFMO can be also attributed to the spin-dependent transfer across these APBs because the domains separated by the APB are couple antiferromagnetically,¹⁶ and the progressive aligning of the antiparallel spins of Fe ions in the APB region by the external field would lead to the high-field magnetoresistance. The SFMO polycrystalline with high concentration of antisite defects was found to show a comparable larger HFMR.¹⁵ Moreover, a weak MR up to high field with linear magnetic-field dependence was found in Fe-site-substituted SFMO single crystal.¹⁸

Furthermore, in order to explore the physical origin for the large LFMR effect in SFMO, a lot of investigations on cationic substitution for both Sr and Mo ions have been extensively reported,^{19–22} but less work has been done about doping at Fe site, which should be more helpful for understanding the correlation between magnetic structure and transport properties in SFMO. However, it was shown that the degree of cation ordering, magnetic, and transport properties of doped SFMO depended strongly on the dopant species and concentration. For example, the degree of cation ordering, saturation magnetization, and MR in SFMO all decrease by doping Cr (Ref. 23) and V (Ref. 24) at Fe site, in contrast to the case of substituting Mn,²⁵ Al,^{26,27} and Cu²⁸ for Fe, in which the degree of ordering of double-perovskite structure was improved by doping, but only Al doping can enhance the LFMR of this compound.²⁷ Therefore, further research about doping at Fe site in SFMO is still necessary to understand this compound more comprehensively and thoroughly.

In this paper, the structural, magnetic, and magnetoresistance properties of $\text{Sr}_2\text{Fe}_{1-x}\text{Al}_x\text{MoO}_6$ ($0 \leq x \leq 0.30$) polycrystalline were systematically investigated. The Al-doped SFMO samples show a great enhancement of LFMR while their HFMR is reduced by the improvement of cation ordering. It was found that the effect of nonmagnetic Al ions on the magnetoresistance is twofold. For one hand, the HFMR was suppressed due to the decrease of the APBs by introducing Al ions in cationic-disordered regions. On the other hand, it is the paramagnetic Mo–O–Al–O–Mo chains introduced in the cationic-ordered regions that divide the large Mo–O–Fe–O–Mo ferrimagnetic region into some smaller patches and then give rise to the enhancement of the LFMR. Thus, the introduction of some artificial boundaries inside the SFMO crystalline by doping nonmagnetic Al ions at Fe sites should be an approach of enhancing the LFMR effect of SFMO besides modulating the state of grain boundaries.

II. EXPERIMENTAL DETAILS

The polycrystalline bulk $\text{Sr}_2\text{Fe}_{1-x}\text{Al}_x\text{MoO}_6$ samples with $x=0, 0.05, 0.10, 0.15,$ and 0.30 were prepared by solid-state reaction as described in Ref. 27. X-ray diffraction (XRD)

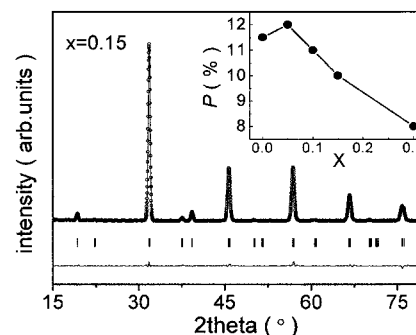


FIG. 1. The experimental (open circle) and calculated (solid line) patterns of room-temperature x-ray powder diffraction for the $x=0.15$ sample. Their difference (solid line on the bottom) is also shown. (The Rp and the Rwp are 8.5% and 9.7%, respectively.) The variation of the degree of cationic disorder p with Al content x is shown in the inset of Fig. 1.

powder patterns were collected using the Bede D¹ XRD spectrometer with Ni-filtered Cu $K\alpha$ radiation. The room-temperature XRD patterns were refined by the Rietveld method using the program FULLPROF.²⁹ The surface morphology of samples, observed by the Hitachi S-4700 field-emission scanning electron microscope, showed that the distributions of Al in the doped samples are uniform and not segregated.²⁷ Resistivity and magnetization measurements were carried out using the physical properties measurement system (PPMS) of Quantum Design.

III. RESULTS AND DISCUSSION

Figure 1 shows a typical experimental and calculated XRD patterns at room temperature as well as their difference for the sample $x=0.15$. Based on the tetragonal $I4/m$ space group, the room-temperature XRD patterns of all samples within $0 \leq x \leq 0.30$ were well refined. It was identified that all the samples were crystallized in the single double-perovskite structure without any change in the structure of these compounds. The variation of the degree of cationic disorder p , calculated from the refinement results, with doping concentration x was displayed in the inset of Fig. 1. Here, p is defined as $p=100\% \times [B''(\text{Fe}, \text{Al})]/[B'(\text{Fe}, \text{Al}) + B''(\text{Fe}, \text{Al})]$, in which $B'(\text{Fe}, \text{Al})$ and $B''(\text{Fe}, \text{Al})$ correspond to the occupation of Fe and Al ions at B' and B'' sites.¹² It can be seen from the inset of Fig. 1 that p decreases from 11.5% to 8.0% as increasing the concentration of Al from 0 to 0.3; i.e., the degree of cationic order was progressively improved by doping Al ions. Therefore, with the increase of Al concentration, the number of antisite defects will decrease gradually. So the magnetic moment per Fe ion will be changed by the substitution of Al ions for Fe ions in the cationic-disordered regions due to the decrease of antiferromagnetic-coupled Fe–O–Fe pairs.

Figure 2 shows the isothermal magnetization curve of the sample $x=0.15$ at 5 K and magnetic field up to 5 T. The magnetization rises rapidly with the increase of H due to the rotation of the ferromagnetic domains under low field and then nearly saturates above 1 T. Other samples have similar features. The saturation moments per formula unit (M_S) with Al content obtained from these magnetization curves are shown in Fig. 3. The value of M_S in pure SFMO ($3.08\mu_B$) is

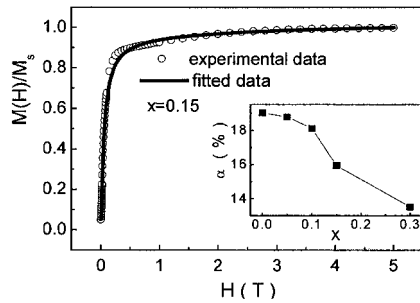


FIG. 2. The isothermal magnetization curve of the sample $x=0.15$ and 5 K up to 5 T. Inset shows the variation of fitting parameter α with Al concentration.

much lower than the theoretical value ($4\mu_B$) as reported in literatures.⁸⁻¹³ It means that this sample has many antisite defects and thus many insulating APB “clusters.”¹⁴ With increasing the Al concentration, the value of M_S in $\text{Sr}_2\text{Fe}_{1-x}\text{Al}_x\text{MoO}_6$ decreases gradually due to partial substitution of Fe^{3+} ions by nonmagnetic Al^{3+} ions. However, it is strange that, with the increase of Al content, the magnetic moment per Fe ion (M_{Fe}) for $\text{Sr}_2\text{Fe}_{1-x}\text{Al}_x\text{MoO}_6$ compounds decreases slightly at $x=0.05$ and then increases notably with increasing the Al concentration. Here, M_{Fe} was roughly calculated from $(M_S+1)/(1-x)$ regardless of the effect of antisite defects because the Mo^{5+} ion ($1\mu_B$) coupled with Fe^{3+} ion ($5\mu_B$) is antiferromagnetically in ordered SFMO structure. It can be seen clearly from Fig. 3 that the value of M_{Fe} at highest doping concentration ($4.76\mu_B$) is much higher than that of undoped sample ($4.06\mu_B$), and nearly close to the theoretical value of magnetic moment of Fe^{3+} ($5\mu_B$). This feature is mainly caused by the decrease of antisite defects of Fe ions by Al doping due to the increase of degree of cationic order and consistent with the result from the XRD refinements.

When two domains, one with Fe at the normal B' site and the other at the antisite B'' site, merge each other, the APBs of Fe–O–Fe would form in SFMO.¹⁴ In these APBs, Fe^{3+} ions couple with each other antiferromagnetically by superexchange interaction (Fe–O–Fe), which not only leads to the reduction of saturation magnetization in SFMO, but also results in the HFMR in this compound due to the spin-dependent transfer (or tunneling) across these APBs. With the increase of the external field, the resistivity for the spin-dependent electron scattering will be reduced gradually due

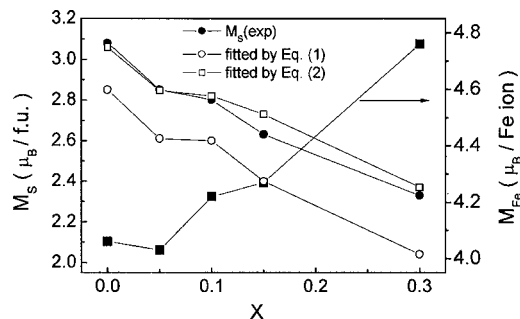


FIG. 3. The dependences of the saturation magnetic moment per formula unit and per Fe ion on x . The fitting results based on different models are also shown.

to progressive rotation of the antiparallel spins of Fe ions in the APB region to the orientation of the external field, and then lead to the HFMR because the antiferromagnetic-coupled spins in APB can usually be aligned under high magnetic field. Therefore, the improvement of cation ordering should suppress the HFMR that will be discussed in detail later.

Accompanied with the formation of antiferromagnetic Fe–O–Fe APBs, the Mo–O–Mo APBs would form in simultaneously SFMO. Two models concerning different coupling ways among Mo ions have been proposed in order to account for the saturation moments per formula unit M_S . In the first case, the Mo ion is assumed to couple with its neighboring Mo ions ferromagnetically,³⁰ and then the value of M_S in pure SFMO is given by $(4-10p)\mu_B$, where p is the degree of the cationic disorder. When Fe ions were partially replaced by Al ions, the value of M_S in $\text{Sr}_2\text{Fe}_{1-x}\text{Al}_x\text{MoO}_6$ would be changed to

$$M_S = [(4-10p) - x(5-10p)]\mu_B, \quad (1)$$

where $(5-10p)$ is the contribution of doping Al to the total magnetic moment. But it was found that this model is not consistent with our experimental data, as shown in Fig. 3 (open circle), where all the values calculated from Eq. (1) are smaller than the experimental data for all samples. In the second case, it was supposed that there is no magnetic coupling within Mo–O–Mo (Ref. 8) based on the fact that the SrMoO_4 exhibits paramagnetic behavior.^{7,13} Then the value of M_S in pure SFMO will be $(4-8p)\mu_B$, which agrees with the Monte Carlo computation on the similar assumptions⁷ and the experimental data obtained by Balcells *et al.*¹⁰ When some Fe ions were replaced by Al ions, the value of M_S in $\text{Sr}_2\text{Fe}_{1-x}\text{Al}_x\text{MoO}_6$ can be given as

$$M_S = [(4-8p) - x(4-9p)]\mu_B, \quad (2)$$

where $(4-9p)$ is also the contribution of doping Al to the total magnetic moment for SFMO. It is clearly seen that this model can fit our experimental data excellently within the whole doping range, as shown in Fig. 3 (open square).

Based on the above analysis, the contributions to total magnetic moment of $\text{Sr}_2\text{Fe}_{1-x}\text{Al}_x\text{MoO}_6$ can be divided into three different parts; i.e., ferrimagnetic-coupled Fe–O–Mo, antiferromagnetic-coupled Fe–O–Fe, and the nonmagnetic-coupled Mo–O–Mo and Mo–O–Al–O–Mo. Then, the normalized magnetization curves of the $\text{Sr}_2\text{Fe}_{1-x}\text{Al}_x\text{MoO}_6$ samples can be fitted by using the following expression:³¹

$$M(H)/M_S = (1-\alpha)[1 - \exp(-H/H_s)] + \alpha \tanh(BH/T), \quad (3)$$

where the first term stands for the contribution of ferrimagnetic-coupled Fe–O–Mo and the second arises from the other three contributions. The prefactor $(1-\alpha)$ refers to the fraction of ferrimagnetic interaction. H_s is the saturated magnetic field and B is an adjustable fitting parameter.^{31,32} The fitting result is shown in Fig. 2 (the solid line). It can be seen that the experimental data for the sample of $x=0.15$ at 5 K up to 5 T can be represented well by Eq. (3). The variation of α with x obtained from the best fits is shown in the inset of Fig. 2. It was found that α decreases monotonously

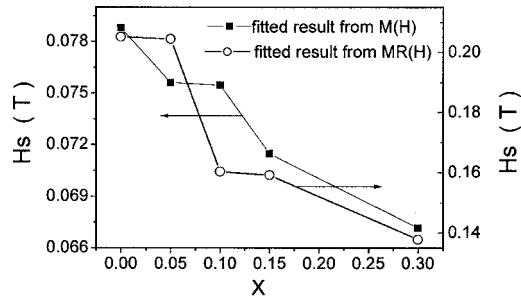


FIG. 4. The variety of H_s based on the fitting of magnetization curves and magnetoresistance curves with different x .

from 19.2% at $x=0$ to 13.5% at $x=0.3$, indicating that the nonferromagnetic contributions of the total magnetic moment in these samples decreases gradually with increasing Al content. Due to the dominant contribution from antiferromagnetic-coupled Fe–O–Fe among the nonferromagnetic contributions, such a decrease of α suggests that the possibility of forming antiferromagnetic Fe–O–Fe pairs was gradually reduced by the substitution of Al for Fe. This result is well consistent with the increased degree of cationic ordering and the enhanced magnetic moment per Fe ion as discussed previously.

The saturated magnetic fields H_s obtained from the best fit of the $M(H)$ curves are shown in Fig. 4 (solid square). It is found that the value of H_s decreases monotonously from 788 Oe at $x=0$ to 670 Oe at $x=0.3$. This means that the magnetic field for aligning the ferrimagnetic domains was reduced progressively with the Al doping. It has been shown previously that the substitution of Al for Fe ions in the cationic-order region of SFMO will give rise to the paramagnetic-coupled Mo–O–Al–O–Mo chains, which divide the original ferrimagnetic Fe–O–Mo region into many smaller patches. Therefore, the magnetic fields, in order to align the smaller, and smaller magnetic regions will decrease gradually with increasing Al content.

Such a reduced magnetic interaction can also be reflected in the temperature dependence of the magnetization. Figure 5 shows the temperature dependence of magnetization for the sample of $x=0.3$ below 120 K at 5 T. Other samples have similar features. It was found that all the experimental data can be well fitted by the Bloch $T^{3/2}$ law,

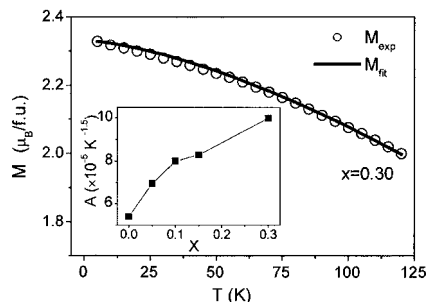


FIG. 5. The temperature dependence of magnetic moment at 5 T below 120 K for the sample of $x=0.3$ and the fitting curve by the Bloch law. The inset shows the variation of the fitted parameter A with doping concentration.

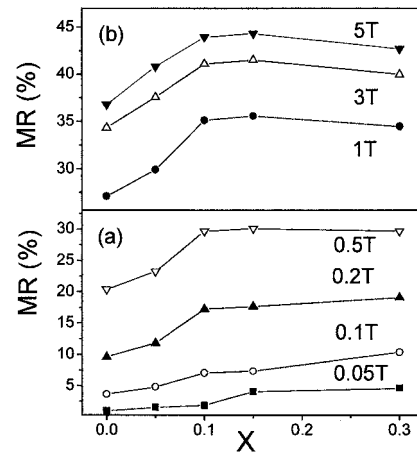


FIG. 6. The variation of MR with Al concentration at 5 K under low field below 0.5 T (a) and high fields up to 5 T (b).

$$M(T) = M(0)(1 - AT^{3/2}), \quad (4)$$

where $A = b(\kappa_B/J)^{3/2}$, b is a constant and J is the exchange integral between the neighboring spins. In our case, it refers to the exchange interaction among the neighboring ferrimagnetic regions. It was found that the fitting parameter A increases, and thus the exchange integral J decreases with increasing Al content as shown in the inset of Fig. 5, which means that the magnetic interaction in ordered regions was weakened gradually with Al doping. This result confirms further the conclusion that the nonmagnetic Mo–O–Al–O–Mo chains in the cationic-ordered region introduced by doping nonmagnetic Al ions will separate the ferrimagnetic Fe–O–Mo region into many smaller patches and thus weaken the interaction among them. In return, these artificial nonmagnetic boundaries formed within the grains through the doping of nonmagnetic Al ions will certainly have strong influences on the spin-dependent carrier scattering and then on the magnetoresistance effect of SFMO.

The variations of MR with Al content x under different magnetic fields up to 5 T at 5 K are shown in Fig. 6, where the MR was defined as

$$MR(\%) = 100\% \times [\rho(0) - \rho(H)]/\rho(0), \quad (5)$$

where $\rho(0)$ and $\rho(H)$ are the resistivity under zero field and external field H , respectively.

It can be seen from Fig. 6 that the MR of SFMO was enhanced remarkably by Al doping in fields below 0.5 T. The MR was increased by 100% at 0.2 T, 200% at 0.1 T, and nearly 360% at 0.05 T. But at high fields over 0.5 T, the magnitude of MR increases rapidly at first, and then decrease slightly beyond $x=0.15$ as shown in Fig. 6(b). This tendency becomes more and more significant with increasing the field. It seems that the increase of MR with Al doping reaches a threshold value at $x=0.15$ under high fields. In terms of the above analysis about the structural and magnetization, the partial replacement of Fe ions by nonmagnetic Al ions in the cationic-ordered regions leads to the formation of the nonmagnetic and insulated Mo–O–Al–O–Mo chains, which separate the original ferromagnetic regions into many smaller ones and act as barriers for spin-dependent carrier

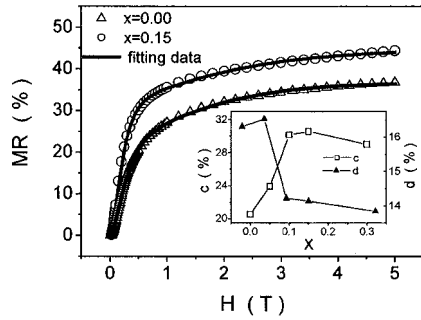


FIG. 7. The magnetic-field dependences of experimental MR data and the fitted data of $x=0.00$ and 0.15 at 5 K up to 5 T. The inset shows the variation of fitting parameters c and d with doping concentration x .

scattering among them. Thus, the LFMR caused by scattering of spin-dependent electrons at these boundaries among the ferrimagnetic regions will be enhanced greatly because their magnetic moments become more sensitive to the external field. Moreover, the HFMR is reduced as the antisite defects and APBs are suppressed by Al doping. Consequently, with increasing Al content, the LFMR will increase gradually but the HFMR decrease gradually, and then the total MR show a maximum at $x=0.15$ under high field.

At last, we will show that the strong correlation between the magnet-transport and magnetic structure of the $\text{Sr}_2\text{Fe}_{1-x}\text{Al}_x\text{MoO}_6$ compounds can be illustrated from the analysis of field dependence of the MR. Xiao *et al.* have demonstrated that the MR originated from the spin-dependent scattering in ferromagnet scales is approximately with the square of normalized magnetization,³³

$$[\rho(H) - \rho(0)]/\rho(0) \approx -A(M/M_s)^2. \quad (6)$$

The low-field MR data of all our samples obey this relationship,²⁷ but their high-field MR data are not accounted for by the above relationship probably due to the presence of nonferromagnetic components including paramagnetic Mo–O–Al–O–Mo and antiferromagnetic Fe–O–Fe besides the ferrimagnetic component as shown in Refs. 12, 15, and 18. In other words, the combined contributions from ferromagnetic and nonferromagnetic regions, which are responsible for the low- and high-field MR, respectively, have to be considered in order to account for the MR of these samples. Thus, we proposed that MR of the $\text{Sr}_2\text{Fe}_{1-x}\text{Al}_x\text{MoO}_6$ samples could be approximately described by the following expression:

$$MR(H) = c[1 - \exp(-H/H_s)]^2 + d \tanh(B \times H/T) \quad (7)$$

in which the first term represent the LFMR arising from the spin-dependent carrier scattering in the ferromagnetic regions and the second term describes the HFMR from the nonferromagnetic components. The value of c and d refer to the MR under low field and high field, respectively. It can be seen from Fig. 7 that the Eq. (7) can excellently describe the experimental magnetic-field dependence of the MR for pure SFMO and $x=0.15$ samples at 5 K and up to 5 T. Others samples that are not shown here all have similar fitting quality. The values of c and d are shown in the inset of Fig. 7. It was found that the value of c increases rapidly from 20.5% at $x=0$ to 30.6% at $x=0.15$, and then changes little beyond x

$=0.15$, while the value of d decreases from 16.3% at $x=0$ to 13.8% at $x=0.3$. This means that the LFMR was enhanced remarkably by Al doping, while the HFMR was suppressed. The competition between them will give rise to the threshold value of $x=0.15$ in the enhancement of MR through Al doping. The variation of H_s obtained from the fitting of the MR (H) curves is also shown in Fig. 4 (open circle). It can be seen that the above H_s shows similar tendency with that from the fitting of magnetization curves. Such an inherent correlation between magnetic and transport properties makes it a potential approach to improve the magnetoresistance through changing the magnetic structures of these double-perovskite materials.

IV. CONCLUSION

In summary, the substitution of nonmagnetic Al ions for Fe ions in SFMO can create some Mo–O–Al–O–Mo chains with no magnetic interaction that can divide the ferrimagnetic Fe–O–Fe domains into some smaller ferrimagnetic ones. This can lead to great enhancement of LFMR of SFMO. Moreover, replacement of Fe ions by nonmagnetic Al ions in the antisite regions could hinder the formation of antiferromagnetic Fe–O–Fe pairs, and then improve the degree of cationic order in SFMO. Consequently, the HFMR of SFMO was suppressed due to the weakness of spin-dependent transfer across the antiphase boundaries or antisite defects. Furthermore, the reversal effect on the magnetoresistance of nonmagnetic Al ions introduced into the cationic-ordered and -disordered regions will give rise to the threshold of $x=0.15$ for enhanced magnetoresistance under field over 0.5 T.

ACKNOWLEDGMENTS

This work was supported by the National Natural Science Foundation of China (Grant No. 10304004).

- ¹A. P. Ramirez, R. J. Cava, and J. Krajewski, *Nature (London)* **386**, 156 (1997).
- ²R. J. Soulen *et al.*, *Science* **282**, 85 (1998).
- ³K.-I. Kobayashi, T. Kimura, H. Sawada, K. Terakura, and Y. Tokura, *Nature (London)* **395**, 677 (1998).
- ⁴C. L. Yuan, S. G. Wang, W. H. Song, T. Yu, J. M. Dai, S. L. Ye, and Y. P. Sun, *Appl. Phys. Lett.* **75**, 3853 (1999).
- ⁵H. Q. Yin, J.-S. Zhou, J.-P. Zhou, R. Dass, J. T. McDevitt, and J. B. Goodenough, *Appl. Phys. Lett.* **75**, 2812 (1999).
- ⁶D. Niebieskikwiat, A. Canciro, R. D. Sánchez, and J. Fontcuberta, *Phys. Rev. B* **64**, 180406 (2001).
- ⁷A. S. Ogale, S. B. Ogale, R. Ramesh, and T. Venkatesan, *Appl. Phys. Lett.* **75**, 537 (1999).
- ⁸M. Garía-Hernández, J. L. Martínez, M. J. Martínez-Lope, M. T. Casais, and J. A. Alonso, *Phys. Rev. Lett.* **86**, 2443 (2001).
- ⁹D. D. Sarma, E. V. Sampathkumaran, S. Ray, R. Nagarajan, S. Majumdar, A. Kumar, G. Nalini, and T. N. Guru Row, *Solid State Commun.* **114**, 465 (2000).
- ¹⁰L. Balcells, J. Navarre, M. Bibes, A. Roig, B. Martine, and J. Fontcuberta, *Appl. Phys. Lett.* **78**, 781 (2001).
- ¹¹R. P. Borges, R. M. Thomas, C. Cullinam, J. M. Coey, R. Ruryanarayanan, L. Ben-Dor, L. Pinsard-Gaudart, and A. Revcolevschi, *J. Phys.: Condens. Matter* **11**, L445 (1999).
- ¹²Y. Tomioka, T. Okuda, Y. Okimoto, R. Kumai, K.-I. Kobayashi, and Y. Tokura, *Phys. Rev. B* **61**, 422 (2000).
- ¹³H. Sakuma, T. Taniyama, Y. Kilamoto, and Y. Yamazaki, *J. Appl. Phys.* **93**, 2816 (2003).
- ¹⁴J. B. Goodenough and R. I. Dass, *Int. J. Inorg. Mater.* **2**, 3 (2000).

- ¹⁵J. Navarro, L. Balcells, F. Sandiumenge, M. Bibes, A. Roig, B. Martínez, and J. Fontcuberta, *J. Phys.: Condens. Matter* **13**, 8481 (2001).
- ¹⁶J. Lindén, M. Karppinen, T. Shimada, Y. Yasukawa, and H. Yamauchi, *Phys. Rev. B* **68**, 174415 (2003).
- ¹⁷T.-T. Fang, *Phys. Rev. B* **71**, 064401 (2005).
- ¹⁸Y. Moritomo, H. Kusuya, T. Akimoto, and A. Machida, *Jpn. J. Appl. Phys., Part 2* **39**, L360 (2000).
- ¹⁹A. Maignan, B. Raveau, C. Martin, and M. Hervieu, *J. Solid State Chem.* **144**, 224 (1999).
- ²⁰J. Lindén, T. Yamamoto, J. Nakamura, H. Yamauchi, and M. Karppinen, *Phys. Rev. B* **66**, 184408 (2002).
- ²¹K.-I. Kobayashi, Y. Kimura, Y. Tomioka, H. Sawada, K. Terakura, and Y. Tokura, *Phys. Rev. B* **59**, 11159 (1999).
- ²²K.-I. Kobayashi, T. Okuda, Y. Tomioka, T. Kimura, and Y. Tokura, *J. Magn. Magn. Mater.* **218**, 17 (2000).
- ²³X. M. Feng, G. H. Rao, G. Y. Liu, H. F. Yang, W. F. Liu, Z. W. Ouyang, and J. K. Liang, *Physica B* **344**, 21 (2004); J. H. Kim, G. Y. Ahn, S.-I. Park, and C. S. Kim, *J. Magn. Magn. Mater.* **282**, 295 (2004).
- ²⁴Q. Zhang, G. H. Rao, X. M. Feng, G. Y. Liu, Y. G. Xiao, Y. Zhang, and J. K. Liang, *Solid State Commun.* **133**, 223 (2005).
- ²⁵X. M. Feng *et al.*, *J. Phys.: Condens. Matter* **14**, 12503 (2002).
- ²⁶A. Peña, J. Gutiérrez, L. M. Rodríguez-Martínez, J. M. Barandiarón, T. Hemández, and T. Rojo, *J. Phys.: Condens. Matter* **13**, 6535 (2001).
- ²⁷Y. Sui *et al.*, *Appl. Phys. Lett.* **85**, 269 (2004).
- ²⁸C. L. Yuan, Y. Zhu, and P. P. Ong, *J. Appl. Phys.* **91**, 4421 (2002).
- ²⁹H. M. Rietveld, *Acta Crystallogr.* **22**, 151 (1967); D. B. Wiles and R. A. Young, *J. Appl. Crystallogr.* **14**, 149 (1981).
- ³⁰A. P. Douvalis, M. Venkatesan, J. M. D. Coey, M. Grafoute, J.-M. Grenèche, and R. Suryanarayanan, *J. Phys.: Condens. Matter* **14**, 12611 (2002).
- ³¹M. Rubinstein, V. G. Harris, B. N. Das, and N. C. Koon, *Phys. Rev. B* **50**, 12550 (1994).
- ³²Y. G. Yoo, S. C. Yu, and W. T. Kim, *J. Appl. Phys.* **79**, 5476 (1996).
- ³³J. Q. Xiao, J. S. Jiang, and C. L. Chien, *Phys. Rev. Lett.* **68**, 3749 (1992).